Development of a Fusion-Based Facial Expression Dataset and a Machine Learning Approach for Emotion Recognition

R. Premananda
Department of Electronics and Communication Engineering, Government Engineering College, Huvina Hadagali, Karnataka, India | Visvesvaraya Technological University, Jnana Sangama, Belagavi, Karnataka, India
rpremananda@gmail.com

Sunil S. Harakannanavar
Department of Electronics and Communication Engineering, Nitte Meenakshi Institute of Technology (NMIT), Nitte (Deemed to be University), Yelahanka, Bangalore, Karnataka, India
sunilsh143@gmail.com (corresponding author)

Nagaraj M. Lutimath
Department of Computer Science and Engineering, Dayananda Sagar Academy of Technology and Management, Bengaluru, Karnataka, India
nagarajlutimath@gmail.com

C. P. Vijay
Department of Computer Science and Engineering, (AI&ML), Vidyavardhaka College of Engineering, Mysuru, India
vijay.cp@vvce.ac.in

Ramesh B. Koti
Department of Electronics and Communication Engineering, KLS Gogte Institute of Technology, Udyambag, Belagavi, Karnataka, India
rameshkoti1984@gmail.com

Received: 31 December 2025 | Revised: 7 February 2026 and 25 February 2026 | Accepted: 27 February 2026

 DOI: https://doi.org/10.48084/etasr.17249

ABSTRACT

Facial Expression Recognition (FER) is a key part of affective computing, where it is still difficult to tell the difference between small changes in facial expressions. Many current FER methods depend on single feature descriptors, which do not always extract the extra structural and texture information that facial expressions have. To overcome this limitation, this paper introduces an adaptive weighted feature-level fusion framework that combines a modified Histogram of Oriented Gradients (HoG), Local Binary Patterns (LBP), and Fast Keypoint Detector with Binary Robust Independent Elementary Features (FKBD). The proposed method assigns discriminative weights to each descriptor instead of directly concatenating features. This lets the fusion process focus on important facial cues and ignore unnecessary ones. The weighted feature representation that comes out of this makes it easier to tell classes apart and makes it more resistant to changes in expression. Multiclass Support Vector Machine (SVM) and k-Nearest Neighbors (KNN) classifiers are used to classify expressions. Experimental validation is performed on standard facial expression datasets, such as the CK+ and FERG DB. The suggested framework achieves 98.74% accuracy with SVM and 95.60% accuracy with KNN, outperforming recent FER methods that use handcrafted features. These results show that using adaptive weighting on complementary descriptors is an effective and computationally efficient way to recognize facial expressions.

Keywords-Facial Expression Recognition (FER); feature fusion; handcrafted features; emotion classification; affective computing

I. INTRODUCTION

Facial Expression Recognition (FER) is a key part of affective computing and human-machine interaction that allows systems to automatically understand how people feel, which can be used in various applications such as behavioral monitoring, assistive technologies, surveillance, and emotion-aware interfaces [1]. Although there has been much progress, reliable FER in the real world is still difficult due to differences in lighting, pose, subject diversity, noise, and small differences between facial expressions [2]. These conditions make it harder to recognize details and make the system less reliable. Preprocessing, feature extraction, and classification are the three main parts of a typical FER system [3]. Normalization and alignment in preprocessing reduce differences, feature extraction can offer useful facial representations, and classification can determine the right expression label [4].

Deep learning methods have improved FER by learning hierarchical feature representations from large datasets [5, 6]. Several studies have shown that deep residual networks and training on multiple datasets make systems more robust [7, 8]. Methods that deal with uncertain expressions and attention-based spatial modeling have further increased performance [9-12]. Some researchers have also suggested lightweight deep models to reduce computational costs while still achieving good results [13, 14]. Deep learning methods usually need large, labeled datasets and a lot of computing power, which causes problems with real-time deployment and robustness. Researchers have investigated hybrid methods that use both hand-crafted and learned features to improve stability and interpretability [15-17]. Recent research has examined explainable FER and micro-expression analysis [18, 19]. These methods offer better recognition performance, but also introduce complexity that increases computational cost, making it difficult to find the right balance between accuracy, speed, and reliability [20, 21].

This work suggests a lightweight adaptive feature-fusion framework that combines complementary handcrafted descriptors to deal with these problems. The modified Histogram of Oriented Gradients (HoG) captures global structural information, the Local Binary Patterns (LBP) captures local texture, and the Fast Keypoint-Based Descriptor (FKBD) encodes structural keypoint information. An adaptive weighting strategy combines these features to make it easier to separate classes while still being fast to compute. The proposed framework was tested on standard FER datasets, achieving good performance for real-time and resource-limited applications.

II. PROPOSED METHOD

This work proposes a new hybrid FER framework based on local LBP-FKBD features and global HoG features. An adaptive weighting scheme is used with a combination of two classifiers (SVM and KNN) to find better class boundaries while reducing false positives. This framework offers higher robustness while working across two datasets, CK+ [11] and FERG DB [22]. Figure 1 shows the proposed architecture.

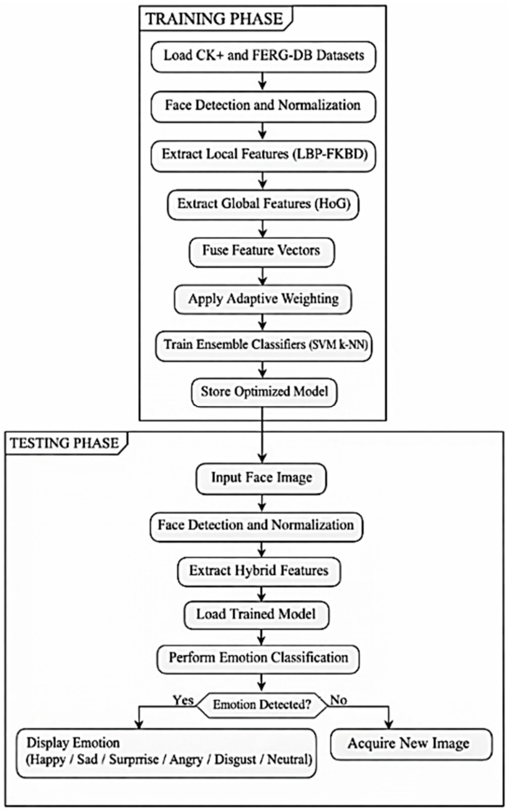

Fig. 1. Proposed model.

The proposed FER system combines feature extraction, an adaptive feature map, and two learning classifiers. It is designed to capture both shallow and dense face patterns, which collaborate and improve the system's accuracy and robustness across different environments. The facial images $I \in R^{H\times W\times C}$ are taken from two highly regarded FER datasets:

- The CK+ (Extended Cohn-Kanade) dataset has 593 real-world sequences from 123 people, with lineups of 7 common faces: Anger, Contempt, Grossness, Fear, Happy, Sad, and Surprise.
- The FERG database features cartoon-like characters with groupings of six recorded faces, suitable for testing over the top and fine expressions.

Histogram equalization and local contrast enhancement were used to homogenize illumination and improve the local contrast, which makes the physical properties of the facial texture associated with an expression more visible, as given in Figures 2 and 3, respectively. The RGB facial image $I(x, y)$ is converted to grayscale to retain structural intensity information as:

$$I_g(x,y) = 0.299\,R(x,y) + 0.587\,G(x,y) + 0.114\,B(x,y) \quad (1)$$

where R, G, B represent the red, green, and blue channels. Let r_k denote the k^{th} gray level with probability [23]:

$$p(r_k) = \frac{n_k}{MN} \quad (2)$$

where n_k is the number of pixels with intensity r_k, and $M \times N$ is the image size. The Cumulative Distribution Function (CDF) is given as [24]:

$$s_k = T(r_k) = \sum_{j=0}^{k} p(r_j) \quad (3)$$

The equalized image is obtained as:

$$I_{eq}(x,y) = (L-1)\, s_k \quad (4)$$

where L is the number of gray levels. Facial landmarks are identified so that the face can be aligned with respect to translation and in-plane rotation [25]. The detected landmarks are represented as:

$$\mathrm{P} = \{(x_i, y_i)\}_{i=1}^{K} \quad (5)$$

An affine transformation is estimated to align the face to a reference template as:

$$\begin{bmatrix} x' \\ y' \\ 1 \end{bmatrix} = \begin{bmatrix} a & b & t_x \\ c & d & t_y \\ 0 & 0 & 1 \end{bmatrix} \begin{bmatrix} x \\ y \\ 1 \end{bmatrix} \quad (6)$$

This normalizes pose, scale, and in-plane rotation [26]. The aligned face is cropped using bounding box limits derived from landmarks as:

$$ROI = I_{eq}(x_1\!:\!x_2,\ y_1\!:\!y_2) \quad (7)$$

This removes background and preserves expression-specific facial regions [27]. Normalization is applied to ensure numerical stability during feature extraction:

$$I_{norm} = \frac{I_{ROI} - \mu}{\sigma} \quad (8)$$

$$I_{norm} \in \mathbb{R}^{H \times W} \quad (9)$$

where μ and σ are the mean and standard deviation of pixel intensities [28]. The output normalized image is forwarded to the feature extractor with a fixed spatial resolution $H \times W$.

(a) (b)

Fig. 2. CK+ sample before (a) and after preprocessing (b) [11].

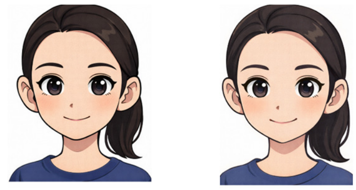

(a) (b)

Fig. 3. FERG DB sample before (a) and after preprocessing (b) [22].

Next, facial landmarks are identified so that the face can be aligned with respect to translation and in-plane rotation. The aligned face is cropped to the Region Of Interest (ROI), which contains facial features that are relevant to the expression, and then is scaled to a predefined size [29]. The normalized picture I_{norm} is passed to the feature extraction module for further processing. To obtain both global and local facial information, three complementary features are taken from each input image:

- Histogram of Oriented Gradients (HoG): Gradient orientation distributions, given in (10), help obtain shape and contour information. HoG is strong against small changes in shape.

$$H_i = \text{HoG}(I_{\text{norm}}), i = 1, \dots, N_H \quad (10)$$

- Local Binary Patterns (LBP): Thresholding is used to encode micro-texture details by looking at the pixels around each center pixel:

$$\text{LBP}_{x,y} = \sum_{p=0}^{P-1} s(I_p - I_c) \cdot 2^p \quad (11)$$

A lightweight FKBD is employed to capture discriminative structural facial patterns [30, 31]. Keypoints are detected using the FAST detector, which identifies high-contrast corner locations in the facial image. Let the detected keypoint set be:

$$K = \{k_i\}_{i=1}^{m} \quad (12)$$

For each keypoint k_i, a binary intensity comparison is performed over predefined pixel pairs within a local patch. The descriptor for the keypoint k_i is defined as:

$$f(k_i) = \sum_{j=1}^{n} \tau(I(p_j^1) - I(p_j^2)) \cdot 2^j \quad (13)$$

where $I(p_j^1)$ and $I(p_j^2)$ represent grayscale intensities at paired pixel locations, and the binary comparison function is used:

$$\tau(x) = \begin{cases} 1, & x > 0 \\ 0, & x \le 0 \end{cases} \quad (14)$$

The final FKBD feature vector is constructed by concatenating descriptors of all detected keypoints using:

$$F_{FKBD} = [f(k_1), f(k_2), \dots, f(k_m)] \quad (15)$$

To ensure numerical stability and scale invariance, the descriptor is normalized using:

$$F_{FKBD}^{norm} = \frac{F_{FKBD}}{\|F_{FKBD}\|} \quad (16)$$

This binary descriptor provides computational efficiency while capturing discriminative structural patterns complementary to HoG and LBP features.

A. Adaptive Weighted Feature Fusion

Let the extracted feature vectors be:

$$F = \{F_{HoG}, F_{LBP}, F_{FKBD}\} \quad (17)$$

Instead of direct concatenation, the proposed method employs adaptive feature-level fusion as:

$$F_{fused} = \sum_{i=1}^{3} \alpha_i F_i, \sum_{i=1}^{3} \alpha_i = 1, \alpha_i \geq 0 \quad (18)$$

The weights α_i are computed analytically using Fisher discriminant optimization to maximize between-class separability while minimizing within-class variance:

$$\alpha^* = \arg\max_{\alpha} \frac{\sum_{c=1}^{C} \| \mu_c - \mu \|^2}{\sum_{c=1}^{C} \sum_{x \in c} \| x - \mu_c \|^2} \quad (19)$$

where μ_c denotes the mean-feature vector of class c, and μ represents the global mean. This optimization enhances discriminative power and suppresses redundant features, improving robustness under illumination and expression variations.

B. Classification

Two classifiers are employed to classify the fused feature vector F_{fused} so that the decisions are complementary.

- Support Vector Machine (SVM) for multiple classes: Finds the best hyperplanes to separate classes of expressions using:

$$\min_{w,b} \frac{1}{2} \| w \|^2 + C \sum_{i=1}^{N} \xi_i \text{ ,s.t. } y_i(w^T F_{\text{fused},i} + b) \geq 1 - \xi_i \quad (20)$$

- k-Nearest Neighbors (KNN): Classifies based on proximity to neighboring samples as given in:

$$\hat{y} = \arg\max_{c \in C} \sum_{i \in N_k} 1(y_i = c) \quad (21)$$

The last prediction is made by either majority voting or confidence-weighted fusion of the outputs from SVM and KNN. This makes the prediction more stable and accurate.

III. RESULTS AND DISCUSSION

All deep learning baselines were set up with ImageNet pretrained weights and then fine-tuned on the FER datasets using the same train/test splits to ensure a fair comparison. Adam optimizer with a learning rate of 1×10^{-4}, a batch size of 32, and early stopping based on validation loss was used for training. To improve the generalizability of the model, data augmentation, such as horizontal flipping, rotation, and changing the lighting, was used. A validation set was used to fine-tune the hyperparameters. Tests were run in MATLAB on the CK+ and FERG-DB datasets. Grayscale conversion, normalization, and facial region extraction were all part of preprocessing. HoG, LBP, and FKBD descriptors were used to extract hybrid features and then combine them through adaptive fusion. Accuracy, precision, recall, F1-score, ROC, and PR curves were employed, along with confusion matrices, to measure performance. A True Positive (TP) is an expression that was correctly classified, a False Negative (FN) is an expression that was missed, a False Positive (FP) is an expression that was incorrectly classified, and a True Negative (TN) is an instance that was correctly rejected. Figure 4 shows the training and validation accuracy of the proposed model over 20 epochs. The training accuracy rises quickly from about 90% to 98.8% in the early epochs, showing that the model learns effectively. The validation accuracy starts lower, at around 88%, but follows the same trend and reaches 98.7%. The small gap between the two curves indicates stable learning and good generalization, with no clear signs of overfitting. Overall, the model converges quickly and maintains high recognition performance. Figure 5 shows the loss of the model over 20 training epochs. The training loss decreases rapidly from 0.34 to below 0.10 in the early epochs and then stabilizes around 0.04, indicating fast convergence. The validation loss follows a similar trend, dropping from 0.46 to about 0.07 and remaining close to the training loss. This behavior indicates effective optimization, minimal overfitting, and good generalization.

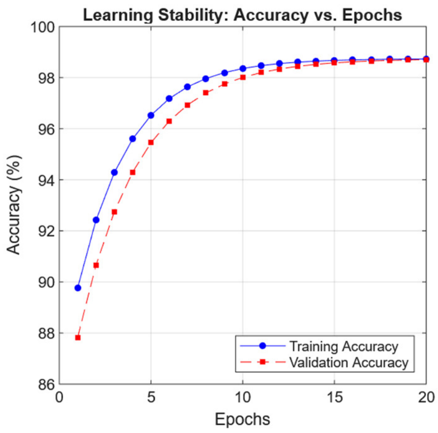

Fig. 4. Plot of accuracy

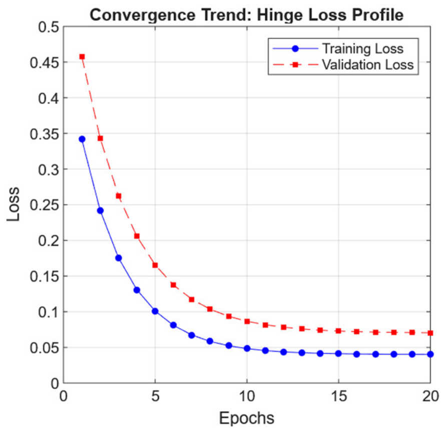

Fig. 5. Convergence trend: hinge loss profile.

The confusion matrix in Figure 6 shows high performance in classifying all seven facial expression classes. Most samples are classified correctly along the main diagonal, with perfect recognition of Disgust, Happy, Sad, and Neutral. Slight misclassifications are noticed for Angry, Fear, and Surprise, with one or two samples each. The low off-diagonal values show that there is little class confusion, and they validate the high discriminability, robustness, and multi-class facial expression recognition capability of the proposed model. Figure 7 shows the accuracy, recall, and F1-score of the model for each emotion class. Most classes get high scores, usually more than 97%, which shows that they do well with all emotions. The model works especially well for expressions of happiness, sadness, and neutrality. Fear and Angry have slightly lower recall, which suggests that the models find it difficult to distinguish the differences between these two similar expressions. The high F1-scores across all classes show that the recognition performance is reliable overall.

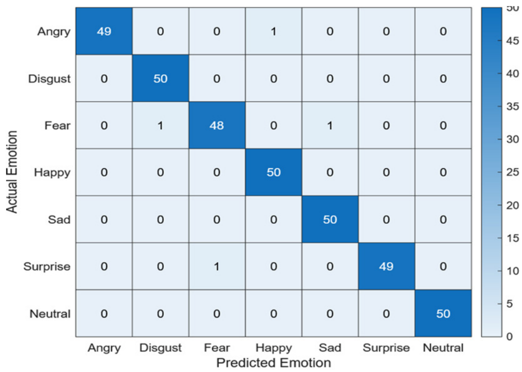

Fig. 6. Confusion matrix

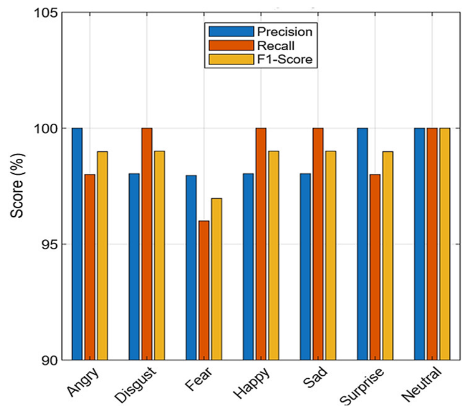

Fig. 7. Detailed analysis per emotion.

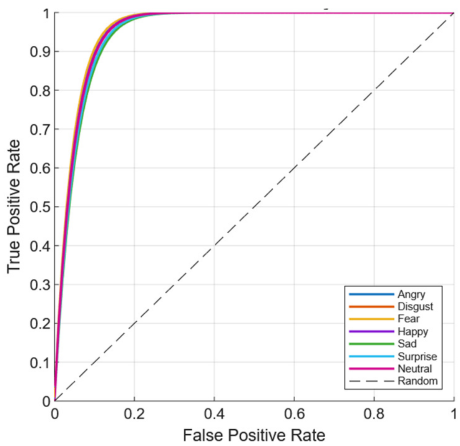

Fig. 8. ROC analysis per emotion.

The multi-class ROC curves in Figure 8 indicate that the proposed FER model achieves a true positive rate exceeding 95% at false positive rates below 10% for all emotion classes. As the false positive rate approaches 20%, the true positive rate rapidly increases to nearly 99–100%, demonstrating high sensitivity. The consistently high TPR values at low FPR levels confirm effective class discrimination and reliable recognition performance across all facial expression categories.

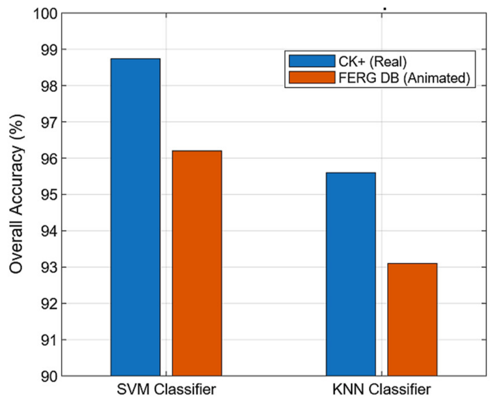

Fig. 9. Cross-dataset performance comparison

Figure 9 compares the performance of SVM and KNN across the CK+ and FERG-DB datasets. The SVM classifier consistently performs better, achieving nearly 99% accuracy on CK+ and about 96% on FERG-DB. In comparison, KNN reaches around 96% on CK+ and 93% on FERG-DB. These results indicate that SVM provides more reliable classification and better generalization across different types of facial expression data.

Figure 10 compares the performance of the proposed FER framework with representative handcrafted and deep learning-based approaches on the CK+ dataset. Traditional handcrafted feature methods, such as LBP and HoG, combined with SVM, typically achieve accuracy in the range of 92–94% on the CK+ dataset. Deep learning models, including CNN-based architectures, generally report accuracy between 95% and 96%. The proposed framework achieves 98.7% accuracy with an F1-score close to 97%, demonstrating improved capability for distinguishing facial expression categories.

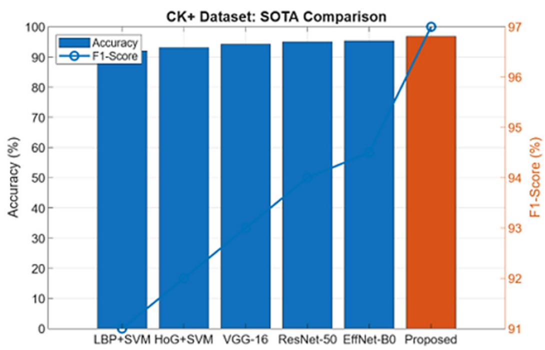

Fig. 10. SOTA comparison on the CK dataset.

On the FERG-DB dataset, traditional handcrafted feature-based approaches typically achieve accuracy in the range of 87–89%, while deep learning architectures generally report performance between 90% and 92%. The proposed method achieves more than 93% accuracy with an F1-score close to 94%, indicating improved recognition capability across different expression groups. The improvement is mainly attributed to the hybrid feature representation and adaptive classification strategy employed in the proposed framework.

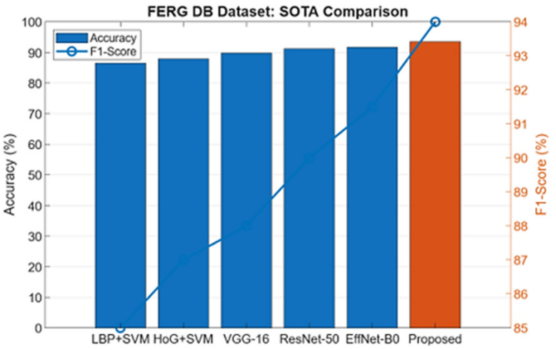

Fig. 11. SOTA comparison on the FERG-DB dataset.

Table I presents the performance of the proposed hybrid FER framework evaluated on the CK+ and FERG-DB datasets. The proposed model achieves 98.7% accuracy with an F1-score of 97% on CK+ and 94% accuracy with an F1-score of 94% on FERG-DB, demonstrating strong recognition performance across both datasets.

TABLE I. PERFORMANCE OF THE PROPOSED FER FRAMEWORK ON CK+ AND FERG-DB DATASETS

Method	**Feature Type / Classifier**	**Dataset**	**Accuracy (%)**	**F1-score (%)**
Proposed model	Hybrid (Deep+Selected features) + ML classifier	CK+	98.7	97
		FERG-DB	94	94

IV. CONCLUSION AND FUTURE SCOPE

This study introduced an adaptive weighted feature-fusion technique for FER by employing HoG, LBP, and FKBD descriptors. The method does not concatenate features but gives each descriptor an analytical weight based on how well it separates different types of data. This makes it easier to separate classes without making the system less efficient. Experiments on the CK+ and FERG-DB datasets showed that the SVM worked well, achieving 98.74% accuracy on CK+, and KNN achieved 95.60% accuracy on FERG-DB. The results show that using adaptive weighting with complementary handcrafted features can improve recognition accuracy without raising the computational cost. Since both CK+ and FERG-DB are controlled datasets, the current evaluation does not accurately reflect real-world conditions. Future work will test the proposed method on real-world datasets, such as RAF-DB and AffectNet, make the method more robust to changes in pose and lighting, and adapt it to recognize spontaneous and micro-expressions.

REFERENCES

[1] J. Liao, Y. Lin, T. Ma, S. He, X. Liu, and G. He, "Facial Expression Recognition Methods in the Wild Based on Fusion Feature of Attention Mechanism and LBP," *Sensors*, vol. 23, no. 9, Apr. 2023, https://doi.org/10.3390/s23094204.

[2] L. Liao, Y. Zhu, B. Zheng, X. Jiang, and J. Lin, "FERGCN: facial expression recognition based on graph convolution network," *Machine Vision and Applications*, vol. 33, no. 3, Mar. 2022, Art. no. 40, https://doi.org/10.1007/s00138-022-01288-9.

[3] S. Wang *et al.*, "GCANet: Geometry cues-aware facial expression recognition based on graph convolutional networks," *Journal of King Saud University - Computer and Information Sciences*, vol. 35, no. 7, July 2023, Art. no. 101605, https://doi.org/10.1016/j.jksuci.2023.101605.

[4] A. Guo, "Enhancing Facial Expression Recognition with Robust CNN Architectures and Adaptive Preprocessing Techniques," *Applied and Computational Engineering*, vol. 100, no. 1, pp. 136–144, Jan. 2025, https://doi.org/10.54254/2755-2721/2025.20426.

[5] D. Ciraolo, M. Fazio, R. S. Calabrò, M. Villari, and A. Celesti, "Facial expression recognition based on emotional artificial intelligence for tele-rehabilitation," *Biomedical Signal Processing and Control*, vol. 92, June 2024, Art. no. 106096, https://doi.org/10.1016/j.bspc.2024.106096.

[6] Y. Zhang, C. Wang, and W. Deng, "Relative Uncertainty Learning for Facial Expression Recognition," in *Advances in Neural Information Processing Systems*, 2021, vol. 34, pp. 17616–17627.

[7] P. Ramdas, S. S. Harakannanavar, S. K. Chikkanna, and V. I. Puranikmath, "Optimizing deep learning models for facial emotion recognition in embedded systems," *Review of Computer Engineering Research*, vol. 13, no. 1, pp. 69–83, 2026.

[8] C. Liang and J. Dong, "A Survey of Deep Learning-based Facial Expression Recognition Research," *Frontiers in Computing and Intelligent Systems*, vol. 5, no. 2, pp. 56–60, Sept. 2023, https://doi.org/10.54097/fcis.v5i2.12445.

[9] D. Song and C. Liu, "A facial expression recognition network using hybrid feature extraction," *PLOS ONE*, vol. 20, no. 1, 2025, Art. no. e0312359, https://doi.org/10.1371/journal.pone.0312359.

[10] Z. Zhao, Q. Liu, and F. Zhou, "Robust Lightweight Facial Expression Recognition Network with Label Distribution Training," *Proceedings of the AAAI Conference on Artificial Intelligence*, vol. 35, no. 4, pp. 3510–3519, May 2021, https://doi.org/10.1609/aaai.v35i4.16465.

[11] P. Lucey, J. F. Cohn, T. Kanade, J. Saragih, Z. Ambadar, and I. Matthews, "The Extended Cohn-Kanade Dataset (CK+): A complete dataset for action unit and emotion-specified expression," in *2010 IEEE Computer Society Conference on Computer Vision and Pattern Recognition - Workshops*, June 2010, pp. 94–101, https://doi.org/10.1109/CVPRW.2010.5543262.

[12] H. Li, Y. Luo, T. Gu, and L. Chang, "BFFN: A novel balanced feature fusion network for fair facial expression recognition," *Engineering Applications of Artificial Intelligence*, vol. 138, Dec. 2024, Art. no. 109277, https://doi.org/10.1016/j.engappai.2024.109277.

[13] G. I. Tutuianu, Y. Liu, A. Alamäki, and J. Kauttonen, "Benchmarking deep Facial Expression Recognition: An extensive protocol with balanced dataset in the wild," *Engineering Applications of Artificial Intelligence*, vol. 136, Oct. 2024, Art. no. 108983, https://doi.org/10.1016/j.engappai.2024.108983.

[14] H. Li, N. Wang, X. Yang, and X. Gao, "CRS-CONT: A Well-Trained General Encoder for Facial Expression Analysis," *IEEE Transactions on Image Processing*, vol. 31, pp. 4637–4650, 2022, https://doi.org/10.1109/TIP.2022.3186536.

[15] X. Wang, T. Zhang, and C. L. P. Chen, "PAU-Net: Privileged Action Unit Network for Facial Expression Recognition," *IEEE Transactions on Cognitive and Developmental Systems*, vol. 15, no. 3, pp. 1252–1262, Sept. 2023, https://doi.org/10.1109/TCDS.2022.3203822.

[16] F. X. Gaya-Morey, S. Ramis-Guarinos, C. Manresa-Yee, and J. M. Buades-Rubio, "Unveiling the human-like similarities of automatic facial expression recognition: An empirical exploration through explainable ai," *Multimedia Tools and Applications*, vol. 83, no. 38, pp. 85725–85753, Nov. 2024, https://doi.org/10.1007/s11042-024-20090-5.

[17] C. Zhu, "A Review of Facial Expression Recognition Based on Convolutional Neural Networks," *Applied and Computational Engineering*, vol. 104, no. 1, pp. 85–90, 2024, https://doi.org/10.54254/2755-2721/104/20241112.

[18] S. Ihsan, I. Adil, A. Zeb, S. Ulhaq, U. Ahmad, and I. A. Khan, "Artificial Intelligence-Based Facial Expression Recognition for Identifying Customer satisfaction on Products," *International Journal on Robotics, Automation and Sciences*, vol. 7, no. 2, pp. 77–85, July 2025, https://doi.org/10.33093/ijoras.2025.7.2.7.

[19] T. Shuai, S. Beng, F. B. Khalid, and R. W. B. O. K. Rahmat, "Advances in Facial Micro-Expression Detection and Recognition: A Comprehensive Review," *Information*, vol. 16, no. 10, Oct. 2025, https://doi.org/10.3390/info16100876.

[20] C. Duan, "A survey of facial expression recognition in the wild," *Applied and Computational Engineering*, vol. 6, no. 1, pp. 98–106, June 2023, https://doi.org/10.54254/2755-2721/6/20230760.

[21] M. Talele and R. Jain, "A Comparative Analysis of CNNs and ResNet50 for Facial Emotion Recognition," *Engineering, Technology & Applied Science Research*, vol. 15, no. 2, pp. 20693–20701, Apr. 2025, https://doi.org/10.48084/etasr.9849.

[22] D. Aneja, A. Colburn, G. Faigin, L. Shapiro, and B. Mones, "Modeling Stylized Character Expressions via Deep Learning," in *Computer Vision – ACCV 2016*, 2017, pp. 136–153, https://doi.org/10.1007/978-3-319-54184-6_9.

[23] Z. Jin, X. Zhang, J. Wang, X. Xu, and J. Xiao, "Fine-Grained Facial Expression Recognition in Multiple Smiles," *Electronics*, vol. 12, no. 5, Feb. 2023, https://doi.org/10.3390/electronics12051089.

[24] A. Babisha, A. Swaminathan, D. Anuradha, C. Gnanaprakasam, and T. Kalaichelvi, "Advancements in Facial Expression Recognition: State-of-the-Art Techniques and Innovations," *International Journal of Intelligent Systems and Applications in Engineering*, vol. 12, no. 19s, pp. 538–546, Mar. 2024.

[25] C. Mejia-Escobar, M. Cazorla, and E. Martinez-Martin, "Towards a Better Performance in Facial Expression Recognition: A Data-Centric Approach," *Computational Intelligence and Neuroscience*, vol. 2023, no. 1, 2023, Art. no. 1394882, https://doi.org/10.1155/2023/1394882.

[26] Shivangini, R. Prasad, A. Rajput, and S. Karsoliya, "A CNN Model for Facial Emotion Recognition," *Journal of Scientific Research and Reports*, vol. 31, no. 8, pp. 653–661, Dec. 2025.

[27] R. K. Sahi, "Classifying Feelings Using Facial Expression Recognition," *International Journal of Intelligent Systems and Applications in Engineering*, vol. 12, no. 4, pp. 3303–3312, Aug. 2024.

[28] H. Yu, "Facial expression recognition with computer vision," *Applied and Computational Engineering*, vol. 37, no. 1, pp. 74–80, 2024.

[29] K. I. K. Jajan and A. M. Abdulazeez, "Facial Expression Recognition Based on Deep Learning: A Review," *Indonesian Journal of Computer Science*, vol. 13, no. 1, Feb. 2024, https://doi.org/10.33022/ijcs.v13i1.3705.

[30] T. Tuncer, S. Dogan, and A. Subasi, "Automated facial expression recognition using novel textural transformation," *Journal of Ambient Intelligence and Humanized Computing*, vol. 14, no. 7, pp. 9435–9449, July 2023, https://doi.org/10.1007/s12652-023-04612-x.

[31] T. Kopalidis, V. Solachidis, N. Vretos, and P. Daras, "Advances in Facial Expression Recognition: A Survey of Methods, Benchmarks, Models, and Datasets," *Information*, vol. 15, no. 3, Feb. 2024, https://doi.org/10.3390/info15030135.